The Sixth Asia-Pacific Conference on
Wind Engineering(APCWE-VI)
Seoul, Korea, September 12-14, 2005

Numerical study of fluctuating aerodynamic characteristics of a square prism in a uniform flow

Shinichi Oka[1] and Takeshi Ishihara[2]

[1] *Fluent Asia Pacific Co. Ltd., 6-10-1, Shinjuku-ku, Tokyo 160-0023, Japan*
[2] *University of Tokyo,2-11-16, Yayoi, Bunkyo-ku, Tokyo,113-8656, Japan*
[1] *oka@fluent.co.jp,* [2]ishihara@bridge.t.u-tokyo.ac.jp

ABSTRACT

In this study, aerodynamic characteristics of square prism in a uniform flow with respect to various angles of attack were investigated using LES turbulence model. As a result, mean forces, drag and lift, mean surface pressure, and mean flow patterns were in good agreement with the wind tunnel tests. It was found that computational domain in the spanwise direction gave strong impacts on fluctuations, drag, lift, and pressure, indicating that spanwise length should be long enough to evaluate quantitatively. Strouhal number of predictions met well with experiments including capturing of the peak. Finally, we proposed an estimation method of fluctuating aerodynamic forces with no spanwise length dependency, and confirmed the validity of the approach using the numerical results.

1. INTRODUCTION

It is important to know aerodynamic characteristics of flow around a rectangle section structure, typically seen in tall buildings and bridges, in wind engineering area. Flow induced vibrations sometimes occurred at a bridges could cause serious damage to the structure. There are various types of aerodynamic problems such as gast, gallopings, vortex-induced vibrations, and aeroacoustics, of which aerodynamic forces are key to the evaluations. Square prism is a tipical shape of rectangle structures, and considerable experimental studies have been accomplished(e.g. Vickery 1966, Otsuki 1978, Bearman 1982) in which it was addressed that aerodynamic forces, drag, lift, and moment, and surface pressure dramatically change when a separated flow generated at front edge reattaches to the body.

Lately, many numerical studies have been reported, and successful to some extent. For example, Tamura(1990) predicted mean drag forces and mean lift forces for various attack angles using DNS, and the predictions met very well with wind tunnel test results, however, no discussion on fluctuations was presented. Hirano et.al.(Hirano 2002) presented predictions of flow around 2:1 rectangular body using LES, resulting good agreement with wind tunnel test results on mean drag force, mean lift force,

and Strouhal number, however, fluctuations, important when aeroacoustics is of interest, were not included in the discussion. LES, calculates large eddies directly while models small eddies, captures unsteady and three dimensional effect, inherent turbulence characteristics, is a good candidate of the prediction approaches on this topic. Many researches have performed and examined predictions of 0 degree angle of attack, however, very few have focused on angle variations, nor discussed fluctuations.

In this paper, LES was used for the calculations of a square prism in a uniform flow. Section 2 describes numerical model and boundary conditions used in the present calculations. Section 3 presents mean aerodynamic forces, mean surface pressure, and flow patterns. Section 4 presents fluctuating aerodynamics as well as Strouhal number. Section 5 presents our proposed estimation method of fluctuating aerodynamic forces that has no spanwise length dependency.

2. NUMERICAL MODEL AND BOUNDARY CONDITIONS

2.1 Governing equations

The governing equations employed in LES model are obtained by filtering the time-dependent Navier-Stokes equations as follows;

$$\frac{\partial \rho \overline{u}_i}{\partial x_i} = 0 \tag{1}$$

$$\frac{\partial}{\partial t}(\rho \overline{u}_i) + \frac{\partial}{\partial x_j}(\rho \overline{u}_i \overline{u}_j) = \frac{\partial}{\partial x_j}\left(\mu \frac{\partial \overline{u}_i}{\partial x_j}\right) - \frac{\partial \overline{p}}{\partial x_i} - \frac{\partial \tau_{ij}}{\partial x_j} \tag{2}$$

Where, $\overline{u}_j$ and $\overline{p}$ are filtered mean velocity and filtered pressure respectively. ρ is density, and τ_{ij} is subgrid-scale stress defined by

$$\tau_{ij} \equiv \rho \overline{u_i}\,\overline{u}_j - \rho \overline{u_i u_j} \tag{3}$$

The subgrid-scale stresses resulting from the filtering operation are unknown, and modeled as follows;

$$\tau_{ij} = -2\mu_t \overline{S}_{ij} + \frac{1}{3}\tau_{kk}\delta_{ij} \tag{4}$$

Where μ_t is subgrid-scale turbulent viscosity, and $\overline{S}_{ij}$ is the rate-of-strain tensor for the resolved scale defined by

$$\overline{S}_{ij} \equiv \frac{1}{2}\left(\frac{\partial \overline{u}_i}{\partial x_j} + \frac{\partial \overline{u}_j}{\partial x_i}\right) \tag{5}$$

2.2 Smagorinsky model

The subgrid-scale turbulent viscosity μ_t is modeled using Smagorinsky model(Smagorinsky 1963). In the Smagorinsky model, the eddy-viscosity is modeled as

$$\mu_t = \rho L_s^2 \left|\overline{S}\right| = \rho L_s \sqrt{2\overline{S}_{ij}\overline{S}_{ij}} \tag{6}$$

Where L_s is the mixing length for subgrid-scales, and defined as

$$L_s = \min\left(\kappa\delta, C_s V^{1/3}\right) \tag{7}$$

where κ is the von Kármán constant, 0.42, C_s is the Smagorinsky constant, δ is the distance to the closest wall, and V is the volume of the computational cell. An order of 0.1 for C_s is widely used in which normally explicit discritization schemes are used. Negative numerical diffusion is generated in explicit discritization schemes whereas positive one is generated in implicit schemes employed in this study. Therefore, in this study C_s =0.032 is used based on a study in which spectrum approach was applied to a LES calculation (Ma 2000).

2.3 Boundary conditions

Shear stresses are specified for the surfaces of the square prism. When a wall-adjacent cell is in the laminar sublayer, the wall shear stress is obtained from the laminar stress-streain relationship as follows;

$$\frac{\overline{u}}{u_\tau} = \frac{\rho u_\tau y}{\mu} \tag{8}$$

If the mesh is too coarse to resolve the laminar sublayer, it is assumed that the centroid of the wall-adjacent cell falls within the logarithmic region of the boundary layer, and the law-of-the-wall is employed.

$$\frac{\overline{u}}{u\tau_\tau} = \frac{1}{\kappa}\ln E\left(\frac{\rho u_\tau y}{\mu}\right) \tag{9}$$

Where $\overline{u}$ is filtered velocity that is tangential to the wall, u_τ is friction velocity, κ is von Kármán constant, and constant E is 9.8. Inlet boundary is specified as a uniform flow, and outflow is specified for the outlet boundary, and the rest of calculation domain boundaries are specified as symmetry.

2.4 Numerical method

Finite volume method and unstructured collocated mesh approach is used in the calculations. In the governing equation, second order central difference scheme is used for the convective and viscosity term discritization. Second order implicit scheme is used for the unsteady term. SIMPLE(Patanker 1980) method, a semi-implicit approach, is used for solving the discritized equations. The discritized equations are expressed as the followed form.

$$a_p\phi_p = \sum_{nb} a_{nb}\phi_{nb} + b_\phi \tag{10}$$

Where a_p, a_{nb} denote respectively unsteady term, convective term, and diffusion term of the conservation equations. nb, neighboring point, is denoted each cell points of the adjacent cells. FLUENT(Fluent Inc. 2003) was used for the solver.

2.5 Modeling conditions

Each edge length of the square prism is 1 cm. Length of calculation domain, square section as shown in Figure 2, is 60D as shown in Figure 2. Uniform velocity, U, at inlet boundary condition is

15 m/s . Figure 3 shows the grid mesh in the vicinity of the square prism and of a corner of the square prism. As shown in Figure 3, mesh density is higher for the corner and total 62 meshes are distributed on an edge. The corners of the square prism were rounded such that the radius of curvature is 1/100 of the square edge length that is the same as that of Tamura(1990). 1/10D was used for each mesh size in the spanwise direction. Main parameters used in the calculations are presented in Table 1. Total twelve cases were performed with respedct to angles of attack, 0, 2, 6, 8, 12, 13, 14, 16, 20, 30, and 45°, for 1D spanwise length model, and total four calculations were performed with respet to angles of attack, 0, 14, 20, and 45°, for the 6D spanwise length model. In addition, for angle of attack 20°, further cases in which spanwise length are 2D, 3D, and 4D were performed for proposed estimation of fluctuating aerodynamic forces mentioned later.

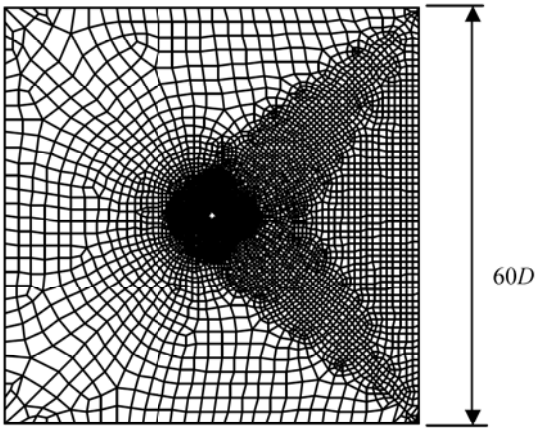

Figure 2. Calculation domain

Table 1. Main parameters

Reynolds num. UD/ν	10^4	
Non-dimensional time tU/D	0.04	
Spanwise length L	1D	6D
Curvature at the corner r	D/100	D/100
Mesh number in span-wise direction N	10	60
Number of the mesh	175,000	1,050,000

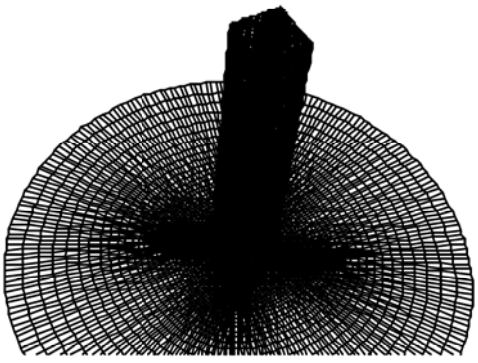

(a) Mesh near the square prism

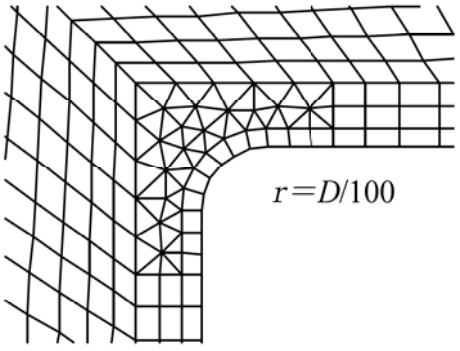

(b) Mesh in the vicinity of edge corner

Figure 3. Mesh in the vicinity of the square prism and its corner

2.6 Definition of coefficients of aerodynamic forces

a. Pressure coefficient

Mean pressure coefficient, $\overline{C}_{pi}$, and fluctuating pressure coefficient, $C_{pi}^{'}$, at i th cell of a square prism surface are respectively defined as follows;

$$\overline{C}_{pi} = \frac{p - p_{ref}}{\frac{1}{2}\rho U^2},\ C_{pi}^{'} = \sqrt{\overline{(C_{pi} - \overline{C_{pi}})^2}} \tag{11}$$

Where, p_{ref} is the reference pressure at mid point in span direction of the lowest corner of the inlet boundary. τ is shear stress, A is surface area of the prism, ρ is reference density, U is reference velocity used inflow velocity. Mean pressure coefficient is derived that taking average of non-dimensional time, tU/D, from 200 to 600 then taking average those data in spanwise direction. The same manner was taken for mean drag and lift averaging operations.

b. Drag and lift coefficients

Figure 4 shows the definition of angle of attack and responded aerodynamic forces directions. As shown in the figure, 0° of angle of attack is defined that front surface of the square prism is normal to the wind direction, positive value for anti-clockwise direction.

Mean drag coefficient, C_D, and lift coefficient, C_L, and fluctuating drag coefficient, $C_D^{'}$, and lift coefficient, $C_L^{'}$, are defined as follows. Where, A_i is the ith cell surface area of a square prism, A denotes a product of D and L, spanwise length. β_i is an angle between normal direction of a prism surface on which the ith cell is belonged and wind direction. In this study, contribution of shear stress, less than 0.2 %, to the aerodynamic forces, was ignored to compare with experiments that were derived from surface pressure.

$$C_D = \overline{\sum_i C_{pi} A_i \cos\beta_i / A},\ C_L = \overline{\sum_i C_{pi} A_i \sin\beta_i / A} \tag{12}$$

$$C_D^{'} = \sqrt{\overline{\left(\sum_i (C_{pi} - \overline{C_{pi}}) A_i \cos\beta_i / A\right)^2}},\ C_L^{'} = \sqrt{\overline{\left(\sum_i (C_{pi} - \overline{C_{pi}}) A_i \sin\beta_i / A\right)^2}} \tag{13}$$

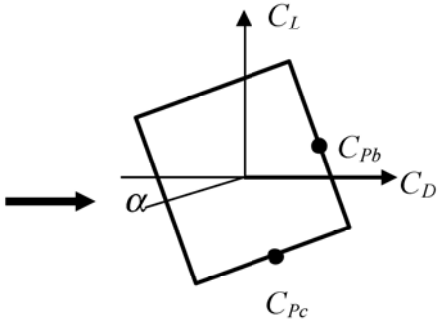

Figure 4. Definitions of aerodynamic forces and angle of attack

3. MEAN AERODYNAMIC FORCES

Mean aerodynamic forces are key factors in gust and galloping problems. How accuracy predictions of those forces is importance. In this section, coefficients of mean aerodynamic forces with respect to various angles of attack are predicted to see characteristics of mean aerodynamic forces. Then mean surface pressure distributions will be derived to find how that is associates with flow patterns.

3.1 Coefficients of mean aerodynamic forces

Figure 5 shows coefficient of mean drag forces and lift forces with respect to attack angles ranging from 0° to 45°. As shown in the figure, in the angles of attack between 0° and 12°, drag coefficient, C_D, moderately decreases with an increase in α, and takes minimum value at around $\alpha = 13°$. At α around 14°, C_D turns to increase and moderately increases with an increase in α greater than 30°. The present calculations were in good agreement with Otsuki(1978) and Igarashi(1984) whereas slightly underestimated at $\alpha = 0°$ and slightly overestimated at $\alpha = 20°$ and 45 ° compared to that of Nishimura(2000). The reason will be mentioned in detail in the later section with which mean surface pressure of the square prism is associated.

Regarding coefficients of mean lift forces, C_L, for angles of attack between 0° and 12°, C_L linearly increases with an increase in α. Angles of attack at around 14°, C_L turns to decreases with an increase in α, and values are almost the same in angles of attack greater than 30°. The prediction results well capture the phenomenon of acute change of mean lift force at around $\alpha = 14°$ that are observed in experiments as well. Overall, predictions of coefficients of mean lift forces are in good agreement with experiments. No significant difference is observed in the results between spanwise length 1*D* case and that of 6*D* case in both mean drag forces and mean lift forces. It can be said that mean aerodynamic forces are quantitatively well predicted using 1*D* of spanwise length, indicating that dependency of spanwise length is small in mean aerodynamic forces.

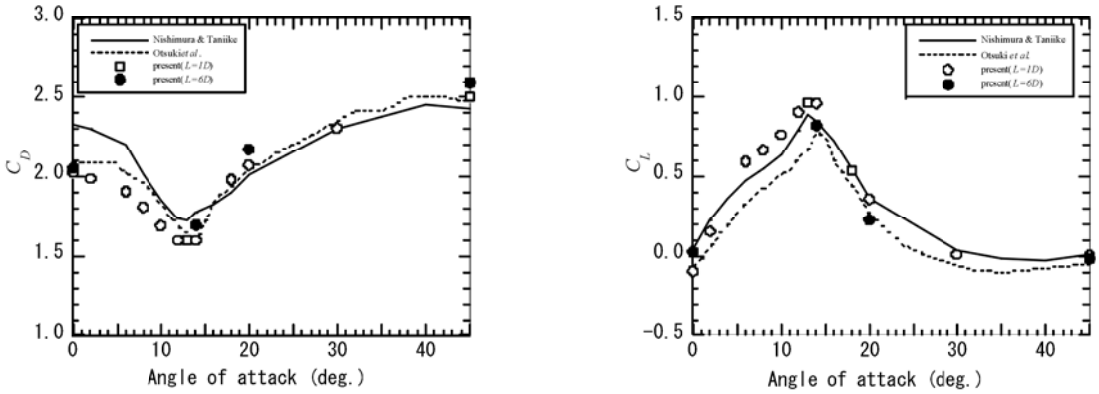

(a) Mean drag forces (b) Mean lift forces

Figure 5. Coefficients of mean drag forces and lift forces

3.2 Mean pressure coefficients

Characteristics of mean aerodynamic forces can be identified by observing mean pressure distributions of the square prism surfaces since mean aerodynamic forces are derived from integration of surface pressures.

Figure 6 shows coefficient of mean pressures, $\overline{C}_p$. At angle of attack at 0°, coefficients of pressure are negative except those in front face, and values are relatively low with small change, indicating that flow pattern is in perfect separation type. As shown in Figure 6(a), predictions of pressure coefficients in the rear surface is over estimated compared to those of experiments. This can be the caused that predictions of drag coefficients underestimate those of Nishimura(2000) as presented in the previous section. At angle of attack 14°, Figure 6(b), pressure recovery in the vicinity of rear edge of the upper surface is observed since magnitude of negative pressure in the vicinity of the rear edge was lower than that in the front edge. It is assumed that intermittent reattachment causes the pressure recovery in this location. Coefficients of pressure at upper surface decreased with an increase in angles of attack, and takes minimum at 14°, that is in good agreement with the experiments. On the other hand, at angle of attack 20°, Figure 6(c), a peak caused by pressure recovery was observed at near rear edge, indicates reattachment of shear layer. For angle of attack at 20° and 45°, rear surface

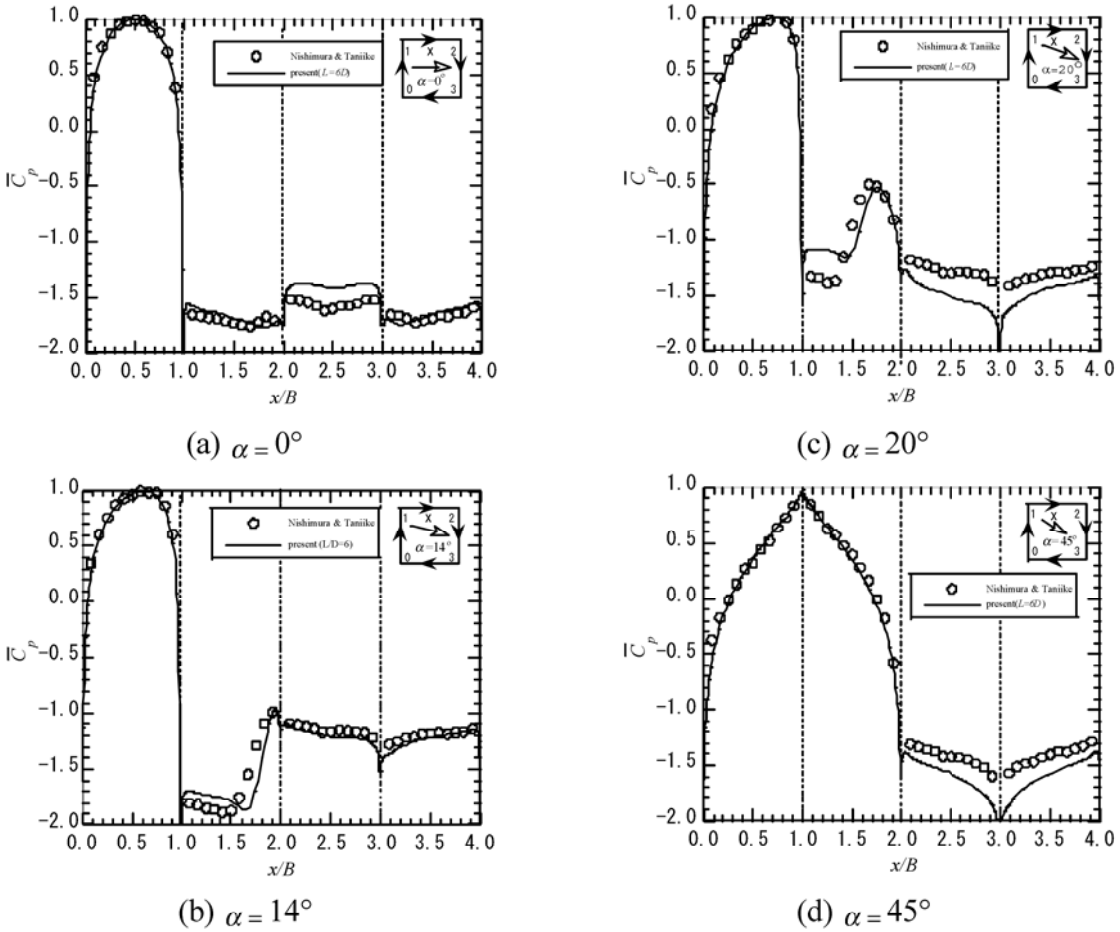

(a) $\alpha = 0°$ (c) $\alpha = 20°$

(b) $\alpha = 14°$ (d) $\alpha = 45°$

Figure 6. Coefficients of surface pressures

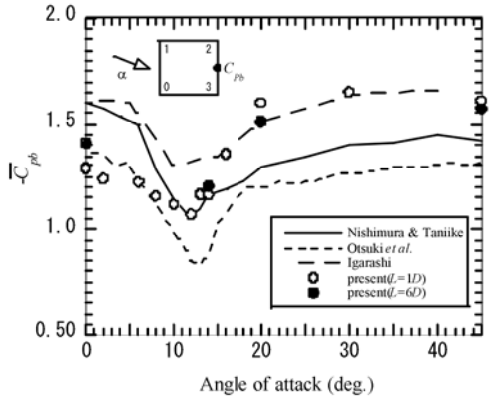

Figure 7. Mean pressure coefficients at the center of rear suface

pressure is underestimated compared to Nishimura(2000), that is caused by that mean drag coefficients are larger than those of their experiment data. Pressures of rear surface depend on behavior of high shear layer in the vicinity of rear corner, and it is possible that extent of the curvature of the corner has impact on the results of both experiments and predictions. Edge length used in the Igarashi is 3 cm of which curvature is relatively large whereas curvatures of Nishimura(2000), 6cm, and Otsuki(1978), 8cm, respectively are relatively small. Impact on the coefficients of mean pressure at the mid rear surface, $\bar{C}_{pb}$, caused by curvatures of square prism corner can be seen in the experiments.

Figure 7 shows mean pressure coefficients at the center of rear surface, $\bar{C}_{pb}$, with respect to the variation of angles of attack. As shown in the figure, the results of predictions were in good agreement with those of Igarashi in which curvature of the corner is relatively large.

3.3 Flow Pattern

Pressure distribution of square prism has large impact on flow patterns. Figure 8 shows mean streamline of four representative attack angles. At angle of attack is 0°, the shear layer form perfect separation flow in which no reattachment to the upper surface of the square prism was observed. Twin large eddies are formed in the back of the square prism. At angle of attack is 14°, Figure 8(b), separated flow at front edge intermittently reattaches at around rear edge. Reattachment area in time average observed in the experiments is well captured. A large singe eddy is formed in the back of the square prism, caused maximum lift force. At angle of attack is 20°, Figure 8(c), separated shear layer clearly reattaches at around rear edge, and separation bubble generated at front edge of the upper surface became small compared to that at angle of attack is 14°. In addition, a single eddy is forming near the lower surface area of the square prism. At angle of attack is 45°, Figure 8(d), streamline goes along with the upper surface, and separated stably at rear edge corner. A twin eddies are formed in the back of the body.

4. FLUCTATING AERODYNAMIC FORCE

From the previous section, mean aerodynamic forces are well predicted using LES. In unsteady aerodynamic force problems and vortex-induced vibration problems, fluctuations of

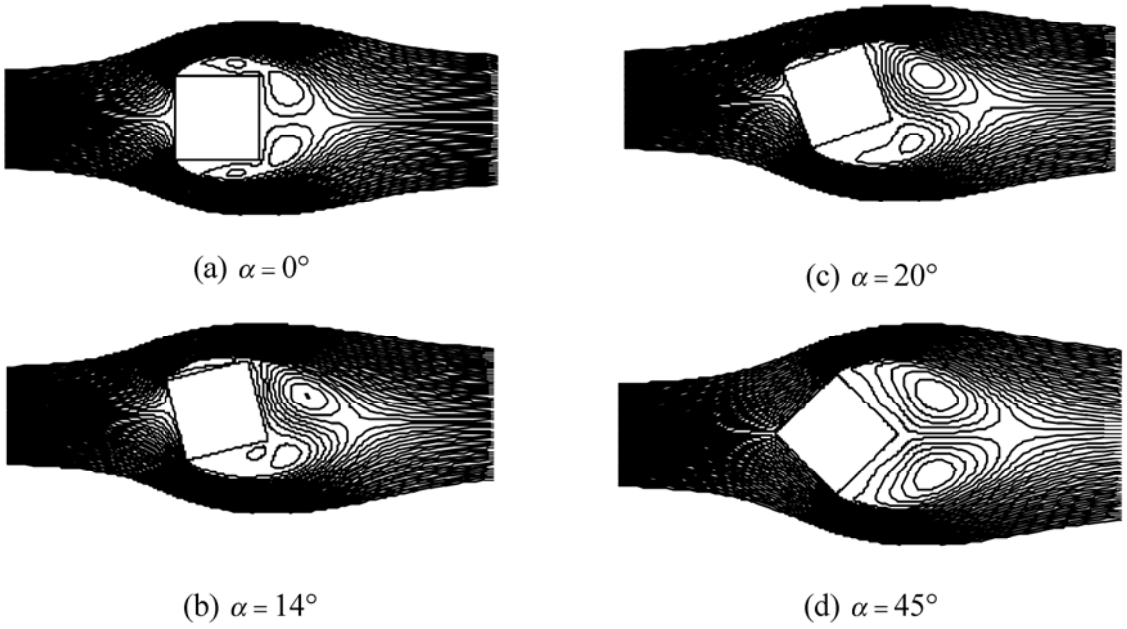

(a) $\alpha = 0°$ (c) $\alpha = 20°$

(b) $\alpha = 14°$ (d) $\alpha = 45°$

Figure 8. Mean streamline in change with angles of attack

aerodynamic forces are of importance. Higher accuracy of high frequency components as well as fluctuations ones are required in a prediction of aeroacoustics problems. In this section, fluctuating aerodynamic forces with varies of angles of attack are investigated.

4.1 Fluctuating aerodynamic forces

Figure 9 shows the results of predictions of fluctuating drag coefficients and fluctuating lift coefficients. As shown in the figure, fluctuations are strongly depend on spanwise length. The results of spanwise length using $6D$ is closer to the experiments compared to that using $1D$.

Regarding fluctuating drag forces, C_D', predictions are in good agreement with the experiments of Nishimura(2000) except that at angle of attack 0° in which prediction is underestimated the experiment.

Regarding fluctuating lift forces, C_L', coefficients of fluctuating lift forces significantly degrease with an incrase in angles of attack between 0° and 8°. Then at angle of attack 12° or greater, C_L' moderately increases until 20° followed by almost flat for angles of attack greater than 20°. This tendency meets the experiments, however, predictions are overestimate the results of Nishimura(2000) in the range of angles of attack larger than 20°. The reason of the overestimation is considered to be the difference between the curvature of the edge corner of numerical model and experiment one.

4.2 Fluctuating pressure coefficients

Fluctuations of pressure coefficients of rear surface and lower surface have strongly affect fluctuations of lift coefficients. Thus at the beginning, those values are derived before discussing the fluctuating pressure coefficients of the square prism.

Figure 10 and Figure 11 respectively show fluctuating pressure coefficients at rear surface center, C'_{pb}, and those of lower surface center, C'_{pc}, plotted with experiments. As shown in figure, predictions of C'_{pb} met well with Igarashi(1984) in all angles attack whereas those are overestimated Nishimura(2000) and Otsuki(1978) for angle of attack greater than 20°. Regarding C'_{pc}, similar trend is observed between predictions and experiments. The reason of the overestimation is considered to be the difference between the curvature of the edge corner of numerical model and experiment one. High-shear layer tends to be unstable in smaller curvature, which means smaller acute angle, and and fluctuations of pressure component of Strouhal number become small.

Figure 12 presents fluctuation of pressure coefficients. Row fluctuation data are non-dimensionalized by dividing C'_{pc} to eliminate the curvature effect mentioned above. At angle of attack 0°, Figure 12(a), the results of predictions were in good agreement with the Nishimura(2000), except rear edge of the upper and the lower surface area where part of the separated shear layer reversely flows and reattaches at the vicinity of rear edge.

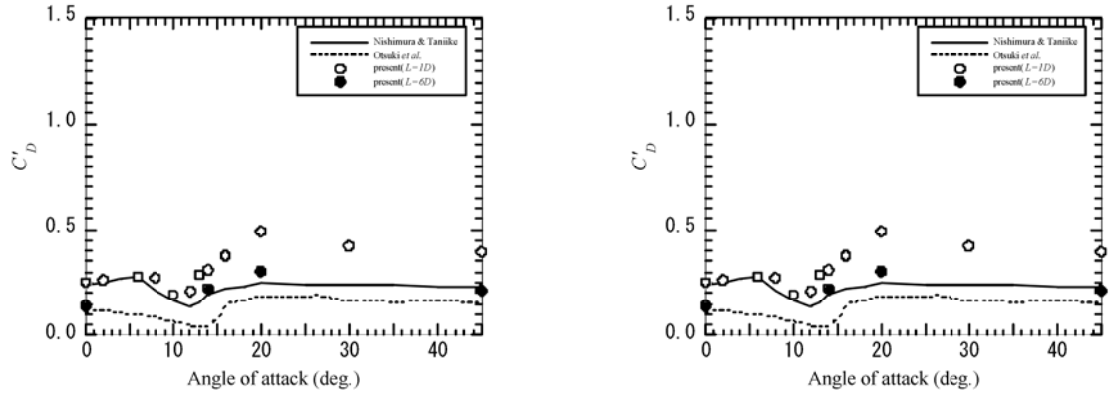

(a) Coefficient of fluctuating drag force (b) Coefficient of fluctuating lift force

Figure 9. Coefficients of fluctuating drag and lift force with angles of attack

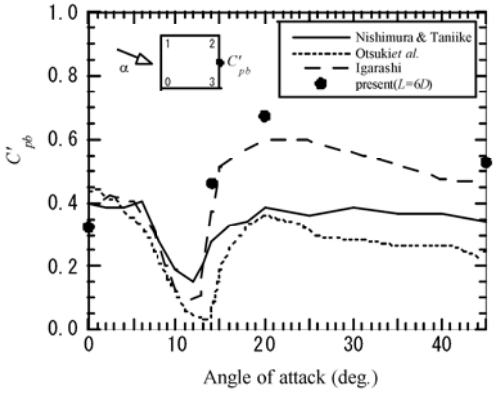

Figure 10. Coefficients of fluctuating pressure at rear face center

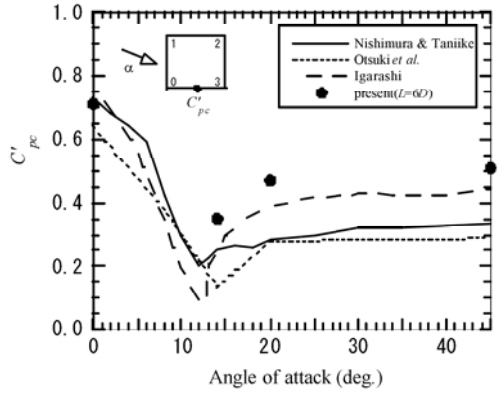

Figure 11. Coefficients of fluctuating pressure at lower face center

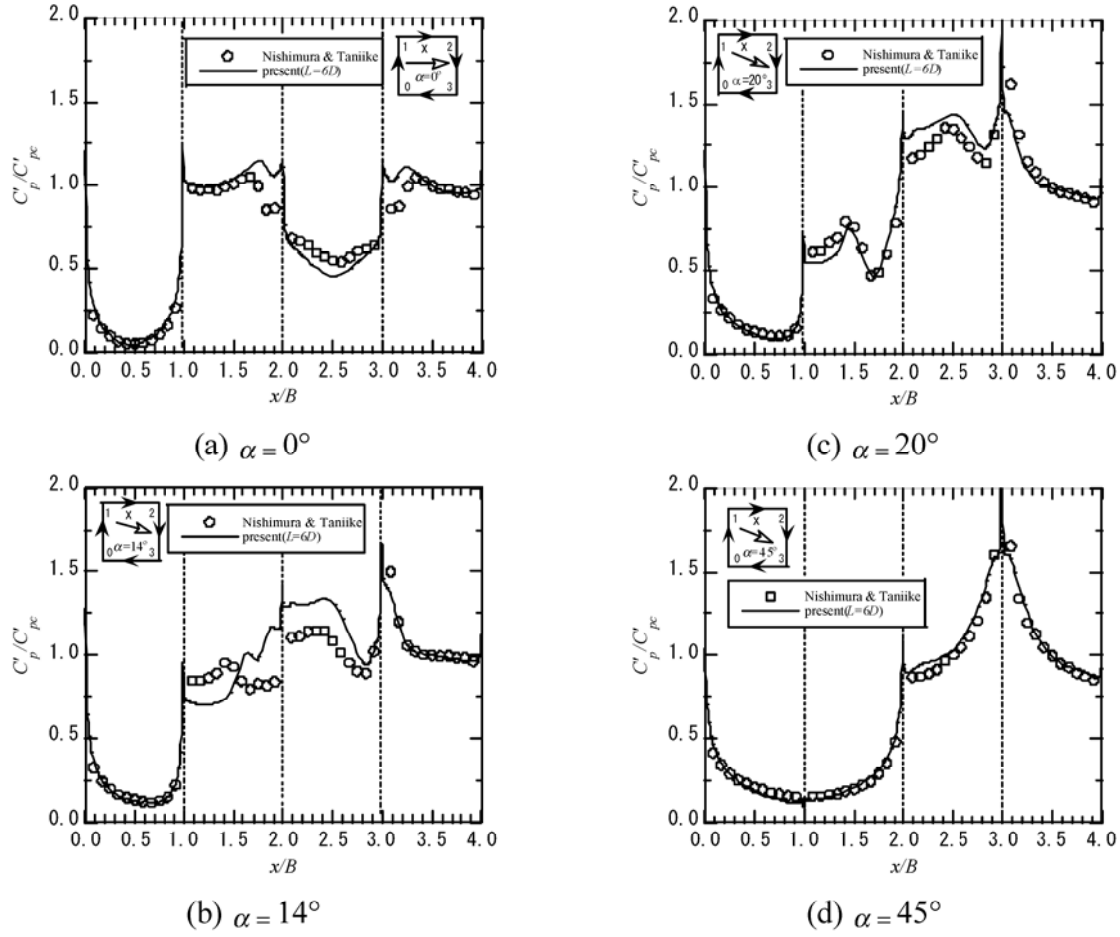

(a) $\alpha = 0°$ (c) $\alpha = 20°$

(b) $\alpha = 14°$ (d) $\alpha = 45°$

Figure 12. Non-dimensionalized pressure distributions

4.3 Strouhal number

Strouhal numbers with respect to each angles of attack are discussed in this section. Figure 13 shows Strouhal number, S_t, defined by $S_t = f_s D / U$. Where f_s is the dominent

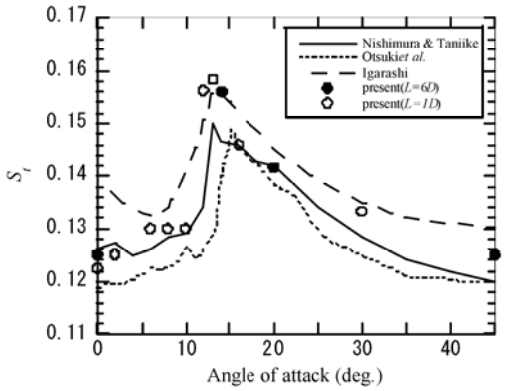

Figure 13. Strouhal number in various angles of attack

frequency of the fluctuating lift force coefficient, D is the length of edge of the square prism, and U is inflow velocity.

As shown in figure, the present calculations qualitatively met well with experiments including capturing the acute change at around 13°. All predictions were in the range of experiments data. It was reported that frequency of vortex shedding at a perfect separation type flow is associated with interference between separation shear layer and wake(Igarashi 1984). In this study, frequencies of vortex shedding are well predicted in both perfect separation type flow and reattachment type flow. According to the results, it can be said that LES, unsteady 3 dimensional model, is able to quantitatively predicts vortex shedding generated from a square prism.

5. A PROPOSAL OF ESTIMATION METHOD OF AERODYNAMIC FRORCES

Aerodynamic forces, fluctuations in particular, depend on length in spanwise direction as mentioned above. In this study, we propose a method for estimating coefficients of aerodynamic forces that do not depend on spanwise length of the square prism. Then we verify the method.

Figure 14 shows coefficients of fluctuations of aerodynamic forces with respect to each span length. By inspection, errors of the predictions decrease monotony as the length is getting longer. Here, we estimate aerodynamic forces, Φ , free from spanwise length using the following equation.

$$\Phi = \phi_\gamma + \varepsilon_\gamma \tag{14}$$

Where, γ is a length factor so that $L = \gamma D$, ϕ_γ is the result of the calculation, ε_γ is predicted errors. Suppose that if a predicted error monotony decreases, prediction error can be approximate as an exponential function.

$$\varepsilon_\gamma = \beta e^{-c\gamma} \tag{15}$$

Where, c is a decay factor, β is a proportional coefficient. Based on the above, coefficients of aerodynamic forces that do not depends on spanwise length is estimated as;

$$\Phi = \phi_\gamma + \beta e^{-c\gamma} \tag{16}$$

Where, γ is an arbitrary positive integer other than zero, and the following equation is derived.

$$\Phi = \phi_\gamma + \beta e^{-c\gamma} = \phi_{\gamma+1} + \beta e^{-c(\gamma+1)} = \phi_{\gamma+2} + \beta e^{-c(\gamma+2)} \tag{17}$$

The proportional coefficient, β , and the decay factor, c, can be derived from Eq.(17) as follows;

$$\beta = \frac{\phi_{\gamma+1} - \phi_\gamma}{1 - e^{-c}} e^{c\gamma} \tag{18}$$

$$c = \ln \frac{\phi_{\gamma+1} - \phi_\gamma}{\phi_{\gamma+2} - \phi_{\gamma+1}} \tag{19}$$

Similar approach is seen in Richardson interpolation method (Richardson 1910) in which discretization errorr of partial differential equations are estimated. In this study, we used power function rather than exponential function Richardson interpolation method employed since the

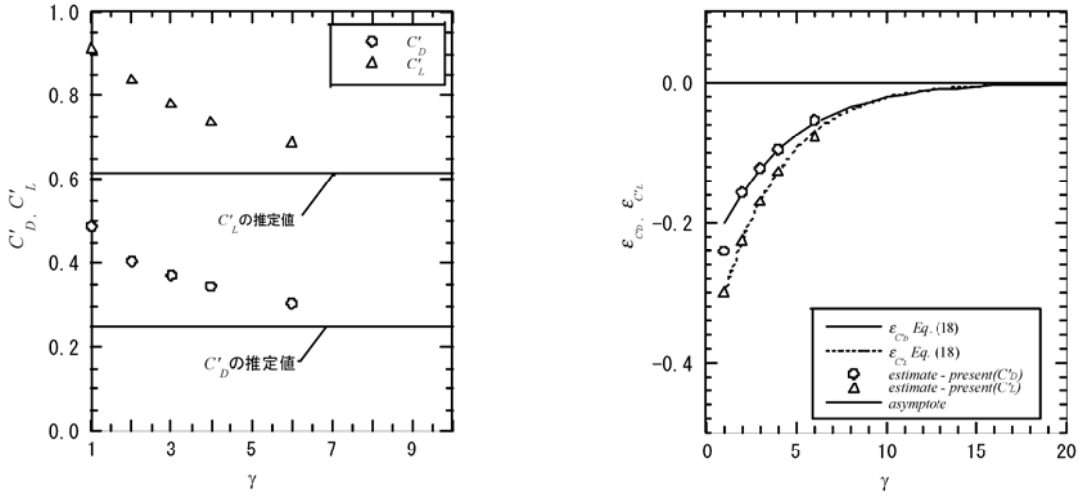

(a) Coefficients of fluctuating aerodynamic forces (b) Estimated errors

Figure 14. Coefficients of fluctuating aerodynamic forces and estimated errors with varying spanwise length

longer the spanwise length the smaller the correlation factor of turbulence exponentially (Wooton 1971). To validate the proposed method, estimated coefficients of fluctuating aerodynamic forces are derived using spanwise length 2*D*, 3*D*, and 4*D*. The results are shown in Figure 14(a).

As seen in figure, coefficients of fluctuating aerodynamic forces are getting closer to the asymptotes as longer the spanwise length. Figure 14(b) shows estimated error with varying spanwise length. Estimated error is getting smaller as spanwise length is getting longer. At spanwise length 20*D*, estimated errors of fluctuating aerodynamic forces become almost zero. As indicated above, it is possible to estimate aerodynamic forces using predictions of spanwise length 2*D*, 3*D*, and 4*D*, resulting a possibility of saving computational costs, smaller calculations time and memory.

6. CONCLUSIONS

Aerodynamic characteristics of square prism in a uniform flow with respect to various angles of attack are investigated using LES turbulence model compared with experiments. As a result the following finings were derived.

1) Regarding coefficients of mean aerodynamic forces, C_D and C_L, and coefficients of mean pressure distributions, $\overline{C}_p$, predictions were in good agreement with experiment in any angles of attack.
2) Regarding coefficients of fluctuations, $C_D^{'}$ and $C_L^{'}$, it was found that predictions heavily depended on domain length in spanwise direction. Coefficients of fluctuating aerodynamic forces are within the range of experiments dispersions. Predictions of coefficients of pressure distributions met well with experiments except the case of angle of attack 14 at which intermittent reattachment is observed in the experiments.
3) Regarding strouhal numbers, acute change with respect to angles of attack was well captured, and the predictions are in good agreement with the experiments.
4) We proposed an estimation method of spanwise length free aerodynamic forces based on shorter

spanwise length square prisms prediction results by changing the spanwise length systematically. In the valiations, spanwise length 4*D* is found to be enough for the estimation of fluctuating aerodynamic forces whereas, normally, 20*D* spanwise length is required.

ACKNOWLEDGMENTS

Authors would like to thank to Dr. Akihiro Nishimura for us to share his valuable experiments data in this study.

REFERENCES

Bearman, P. W., Obasaju, E. D. (1982): "An experimental study of pressure fluctuations on fixed and oscillating square-section cylinders", *J. Fluid Mech.*, Vol. 119, pp. 297-321. Fluent Inc, (2003), FLUENT 6.1 Users Guide.

Hirano, H., Maruoka, A., Watanabe, S. (2002): "Calculations of aerodynamic peroperties of rectangular cylinder with slenderness ratio of 2:1 under various angles of attack", *Journal of Structural Engineering*, Vol. 48A, pp. 971- 978.

Igarashi, T. (1984): "Characteristics of the flow around a square prism", *Bulletine of JSME*, Vol.27, No.231, pp. 1858-1865.

Ma, X., Karamanos, G. S., Karniadakis, G. E. (2000): Dynamics and low-dimensionality of a turbulent near wake, *J. Fluid Mech.*, Vol. 410, pp. 29-65.

Nishimura, A., Taniike, Y. (2000): "Fluctuating wind forces of a stationary two dim. square prism", *Proceedings of 16th National Symposium on Wind Engineerin*g, pp. 255-260.

Otsuki, T., Fujii, K., Washizu, K., Ohya, A. (1978): "Wind tunnel experiments on aerodynamic forces and pressure distributions of rectangular cylinders in a uniform flow", *Proc., 5th Symp. on Wind Effects on Struct.*, pp. 169-176.

Patanker, S.V. (1980): Numerical heat transfer and fluid flow, *McGraw-Hill*, New York.

Richardson, L. F. (1910): "The approximate arithmetical solution by finite differences of physical problems involving differential equations with an application to the stresses in a masonry dam", *Trans. Roy. Soc. London,* Ser. A, Vol. 210, pp. 307-357.

Smagorinsky, J. (1963): "General circulation experiments with the primitive equations. I. The basic experiment", *Month. Wea. Rev.*, Vol. 91, pp. 99-164.

Tamura, T., Ohta, I., and Kuwahara,K. (1990): "On the reliability of two-dimensional simulation for unsteady flows around a cylinder-type", *J. Wind Eng. and Indus. Aerodyn.*, Vol. 35, pp. 275-298.

Vickery, B. J. (1966): "Fluctuating lift and drag on a long cylinder of square cross-section in a smooth and in a turbulent stream", *J. Fluid Mech.*, Vol. 25, pp. 481-494.

Wooton, L. R. and Scruton, C. (1971): "Aerodynamic stability, The modern design of wind-sensitive structures", *CIRIA seminar*.